MATHEMATICAL MODELING AND COMPUTING, Vol. 7, No. 2, pp. 322–333 (2020)

Modeling Computing Mathematical

Giant magnetoresistance effect in InSe⟨β-CD⟨$FeSO_4$⟩⟩ clathrate

Klapchuk M. I.[1], Ivashchyshyn F. O.[1,2]

[1] *Lviv Polytechnic National University,*
12 S. Bandera Str., 79013, Lviv, Ukraine
[2] *Czestochowa University of Technology,*
17 Al. Armii Krajowej, 42-200, Czestochowa, Poland

(Received 24 May 2020; Revised 28 July 2020; Accepted 29 July 2020)

The InSe⟨β-CD⟨$FeSO_4$⟩⟩ clathrate with hierarchical architecture reveals a giant magnetoresistive effect and extraordinary (oscillating) behavior of the current-voltage characteristics in the magnetic field in the direction perpendicular to nanolayers. A new technological approach for the synthesis of multilayered nanostructure is proposed. It allows attaining a fourfold degree of expansion of the initial InSe semiconductor matrix in which the cavitate of β-cyclodextrin (β-CD) and iron sulfate served as a guest content. This makes it possible to develop a theoretical model to describe the interlayer magnetoconductivity in such extremely anisotropic 2D layered compounds. Graphic dependencies of oscillating magnetoconductivity are analysed for different values of quantizing magnetic field in a layered structure whose interlayer transfer integral can be controlled artificially.

Keywords: *InSe, intercalation, clathrate, hierarchical structures, impedance spectroscopy, giant magnetoresistive effect.*

2010 MSC: 82D15, 82D20 **DOI:** 10.23939/mmc2020.02.322

1. Introduction

The giant magnetoresistance effect (GMR), first discovered [1] in 1988, has attracted great attention in recent years as it has greatly influenced the study of magnetic information storage devices [2–5], such as ultra-sensitive magnetic field sensors, reading heads, memristors [6, 7]. In 2007, the Nobel Prize in Physics was awarded to scientists Peter Grünberg and Albert Fert for the study of GMR [2]. The keyword in the discovery was "giant" because over a century of history of studying magnetoelectric phenomena, the magnitude of the magnetoresistance did not exceed a few percent.

A giant magnetoresistance effect has been detected in alternate multilayer iron-chrome structures and its mechanism is well understood today. In short, its essence is that in a magnetic field, electrons with spins oriented along it in all layers of iron will feel more resistance and their contribution to the current will decrease. At the same time, electrons with opposite spin are experiencing less resistance, and the current due to them increases significantly. In fact, how many times the indicated increase in current over its decrease will be observed depends on the properties of the substance.

The degree of the GMR effect is usually described by the so-called magnetoresistance ratio (MR), which can be defined as the corresponding normalized difference, i. e.

$$MR = (G_P - G_{AP})/G_{AP},$$

where G_P and G_{AP} mean conductances of the P (parallel) and AP (anti-parallel) alignments, according to the orientation of the magnetization of adjacent magnetic layers.

The use of the material exhibiting GMR has led to a sharp increase in the density of recording on hard disks. Located over a rapidly rotating hard disk, this structure quickly tracks the magnetic fields of the bits and immediately converts them to electrical current.

The supramolecular ensemble of sub-hosts ⟨host⟨guest⟩-InSe⟨β-CD⟨$FeSO_4$⟩⟩ with magnetic components was successfully synthesized for the first time in our laboratory [8, 9]. In the cited work, the authors analyzed in detail the conductive and polarization properties of the investigated clathrate. However, the explanation of the detected GMR required additional explanation and theoretical substantiation, and this is what the presented work is devoted to.

2. Formulation of the problem

To obtain high MR, an attractive alternative is to use a magnetically confined semiconductor heterostructure. It is a type of hybrid nanostructure consisting of semiconductor and magnetic materials, where nanoscale ferromagnetic bands often settle on the surface of a semiconductor heterostructure and provide a non-uniform magnetic field that locally affects the motion of a two-dimensional electron gas (2DEG) embedded in the semiconductor heterostructure.

All of the above is the basis for highlighting the novelty and benefits of our proposed nanostructure for these purposes. First of all, it should be noted that the traditional approach uses only one of its components to change the conductivity (σ) in a magnetic field, namely its mobility (μ) according to the well-known formula:

$$\sigma = en\mu, \tag{1}$$

where e is the charge of the electron, n is their concentration. In our case, due to the use of semiconductor phases, both the mobility and the concentration of current carriers are responsible for the change in the resistance in the magnetic field. A significant change of the latter is achieved by Zeeman localization or delocalization. This leads to the fact that we can expect not only a significant change in the magnetoresistance but also to observe it at higher temperatures and weaker magnetic fields. Moreover, a new possibility of analyzing the frequency dependence of GMRs opens, since, in general, the resistance of semiconductors is frequency-dependent. This can lead to the creation of functionally hybrid sensors.

3. Materials and methods

To achieve this goal, the third type of substance organization – clathrate (or supramolecular) – was used in view of its structural and energetic features [10–12]. The clathrate InSe⟨β-CD⟨$FeSO_4$⟩⟩ of hierarchical architecture sub-host ⟨host⟨guest⟩⟩ was synthesized by the method of intercalation.

InSe is a layered, black crystal that splits like mica into very thin, smooth, transparent, brown layers with a greenish tinge (Fig. 1). Melting point is 933 K, density 5.560 g/cm^3, microhardness $5.88 \cdot 10^8$ Pa. It is steady in the air and in water. The resistivity, depending on the purity of the sample, varies from 10^2 to 10^4 Ohm·m at $T = 300$ K [13–16]. The sharp maximum of photoconductivity lies at 1.03 μm, which coincides with the edge of the fundamental absorption, which corresponds to the bandgap of 1.20 eV at $T = 300$ K [16, 17]. The basic physical parameters of gallium and indium monoselenides are discussed in [17, 18].

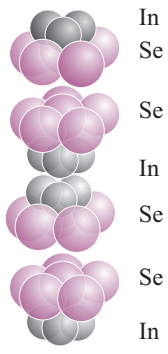

Fig. 1. Spatial image of the structure InSe.

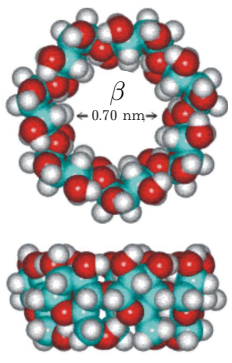

Fig. 2. Structural image of β-CD.

$C_{42}H_{70}O_{35}$ is β-form cyclodextrin (β-CD) (Fig. 2). Its unique structural feature, namely the separation of hydrophilic and hydrophobic groups, causes unusual physical and chemical properties. Most important of these is the ability to re-bind and selectively bind inorganic, organic, biological molecules

to form "lock-key" inclusion complexes. The high electron density inside the β-CD cavity can activate the electrons of the "guest" molecules, leading to changes in the spectral properties of both the incorporated molecules and the β-CD itself [10].

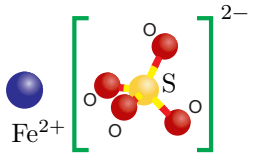

Fig. 3. Chemical formula of iron-sulfate (II).

Iron-sulfate (II) was used as a magnetically sensitive guest component (Fig. 3) [19]. The choice of $FeSO_4$, as a guest component was based on the fact that it is a known precursor for the synthesis of nanomagnetite, as well as the fact that its cationic component has a large spin magnetic moment. This makes it possible to control the properties of encapsulates (for example, the combination of photoelectric and ferromagnetic properties), mainly to ensure their high sensitivity to external physical fields.

Since neither β-CD nor $FeSO_4$ can be directly inserted into InSe, in order to form supramolecular ensembles, we applied the three-stage intercalation-deintercalation technology (Fig. 4), which was described in our previous work [20]. According to this technology, in the first stage, sodium nitrite is introduced into the initial matrix by the method of direct exposure in its melt of a semiconductor single crystal at a temperature of 300°C for $5 \div 10$ minutes. As a result of n-stage ordering, the distance between the respective layers increases significantly. The process was carried out until a 4-fold increase in the thickness of the sample.

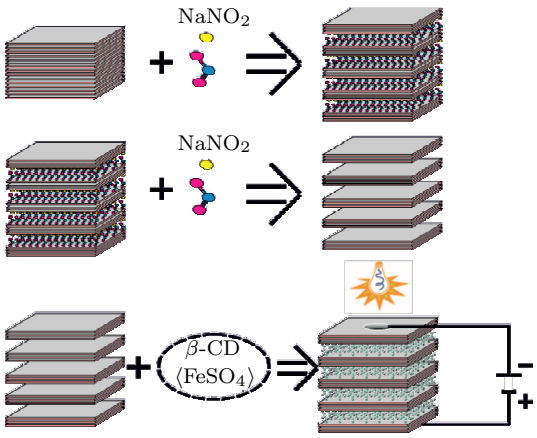

Fig. 4. Stages of InSe$\langle\beta$-CD$\langle FeSO_4\rangle\rangle$ clathrate formation.

The next step was deintercalation of sodium nitrite from the crystal by extracting it over a five-hour 24-hour cycle and drying at 110°C and reduced pressure. Deintercalated matrices have become suitable for the introduction of organic guest components due to weakened van der Waals bonds and modified intracrystalline force fields.

Therefore, in the third stage, β-CD$\langle FeSO_4\rangle$ was intercalated into an expanded crystal lattice by direct exposure in a saturated two-component solution with a molar ratio of β-CD: $FeSO_4$ as a $1:1$ deintercalated matrix at room temperature for 48 hours. In order to provide clathrate functional hybridity and modify the properties during the formation of organic nanolayers in the extended ranges of van der Waals forces InSe, an electric field of 110 V/cm along the crystallographic axis C with simultaneous illumination with visible light was also applied. Next, ohmic contacts were applied to both faces perpendicular to the crystallographic axis (C) of the obtained nanostructure.

The impedance measurements were made in the direction of the crystallographic axis C in the frequency range $10^{-3} \div 10^{6}$ Hz with the help of the "AUTOLAB" measuring complex of the company "ECO CHEMIE" (Netherlands), complete with computer programs FRA-2 and GPES. The amplitude of the measuring signal was $5 \cdot 10^{-3}$ V. The removal of doubtful points was performed by using the Dirichlet filter [21,22]. The frequency dependencies of complex impedance Z were analyzed graphically in the environment of ZView 2.3 software package (Scribner Associates). The approximation errors did not exceed 4%. The correspondence of the constructed impedance models to the experimental data package was confirmed by the completely random nature of the frequency dependences of the first-order residual differences [21,22]. Measurements of impedance dependencies were also carried out in a constant magnetic field (intensity 2.75 kOe) and in a field of light wave (simulator of solar radiation with a power of 65 W) in the direction of their application, namely along the crystallographic axis C. Such a geometry of measurements was chosen to avoid the Lorentz force. The spectra of the thermally stimulated discharge were recorded in the mode of short-circuited contacts under linear heating at a rate of 5° C/min.

4. Results and their discussion

The hierarchy of InSe⟨β-CD⟨$FeSO_4$⟩⟩ clathrate structure leads to the modulation of multibarrier nanosheets, which is confirmed by the appearance of Nyquist diagrams (Fig. 5). It is well evident that the impedance hodograph is a superposition of two arcs, the higher-frequency of which exhibits the current flow in non-intercalated nanosheets and the lower-frequency arc through layers with guest content. At the same time, for each of them, the center lies below the axis of the real component of specific impedance, indicating that there is a certain distribution of relaxation times.

The synthesis of InSe⟨β-CD⟨$FeSO_4$⟩⟩ clathrate in the electric field with simultaneous illumination provides a different nature of the change of the real component of the complex impedance ($\mathrm{Re}\, Z(\omega)$) than during the synthesis under normal conditions. The difference is due to delocalized carriers of the initial matrix providing a fivefold increase in the specific conductivity. The hopping mechanism of conductivity give a significant contribution to the current conduction due to the concentration of trap centers in the vicinity of the Fermi level.

In Fig. 6 the spectra of thermally stimulated discharge of InSe⟨β-CD⟨$FeSO_4$⟩⟩ clathrate are shown. Under the normal conditions, synthesized clathrate is a coordination defect (whose structure is different from the initial matrix) with negative correlation energy, which forms a quasi-continuous spectrum of localized states in the bandgap. Instead, for clathrate synthesized in an electric field with simultaneous illumination, we obtain a wide band of localized states in the band gap. The results of thermally stimulated discharge are in good agreement with the results of impedance spectroscopy.

An interesting result of the measurement of volt-ampere characteristic (VAC) in the constant magnetic field was obtained for InSe⟨β-CD⟨$FeSO_4$⟩⟩ synthesized under the normal conditions (Fig. 7).

It can be represented as a system of N-shaped sections, the occurrence of which is related to the following. It is well known [10, 12] that in quasi-two-dimensional crystals the width of the band $E_\perp$ in the direction perpendicular

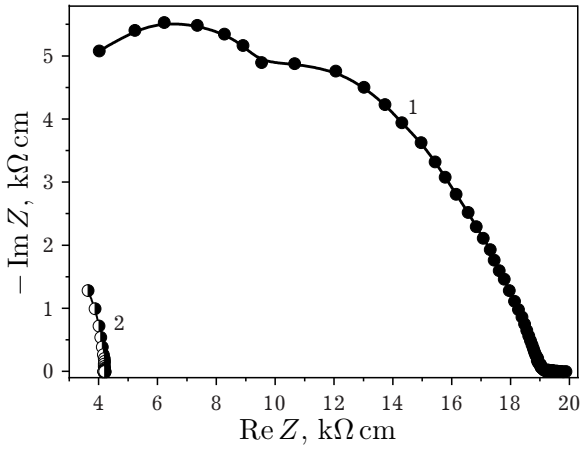

Fig. 5. Nyquist diagrams [8] obtained in the magnetic field for the direction perpendicular to nanolayers in the InSe⟨β-CD⟨ $FeSO_4$⟩⟩ clathrate synthesized under the normal conditions (1) and in the electric field under the simultaneous illumination (2).

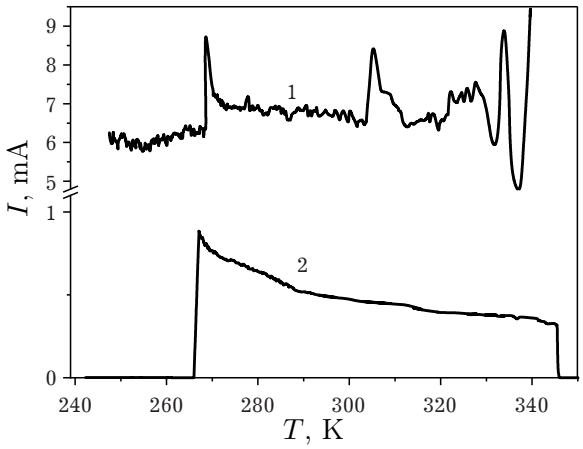

Fig. 6. Currents of thermally stimulated discharge for InSe⟨β-CD⟨$FeSO_4$⟩⟩ clathrate synthesized under the normal conditions (1) and in the electric field under the simultaneous illumination (2).

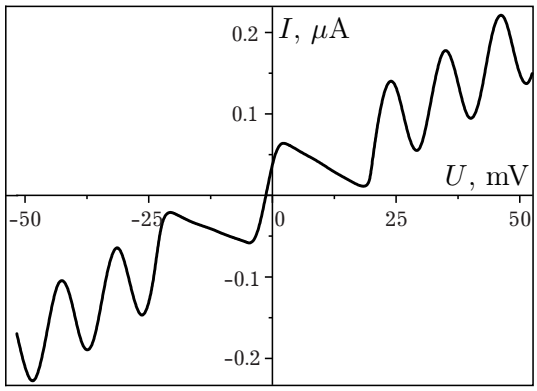

Fig. 7. Volt-ampere characteristic obtained in the magnetic field for the direction perpendicular to nanolayers InSe⟨β-CD⟨$FeSO_4$⟩⟩ nanostructure.

to the layers is small and that it can be substantially reduced by intercalation. In the strong coupling approximation, the dispersion law of such a crystal can be represented as:

$$\varepsilon(p) = \frac{p^2}{2m_{\parallel}} + E_{\perp}\cos(ap_{\perp}).$$

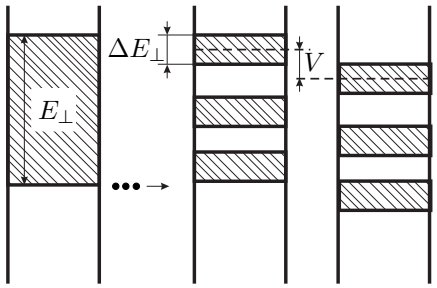

Fig. 8. Sketch of the energy diagram transformation to a mini-band character.

In our case, it is important that the mentioned above continuous band will be transformed to a mini-band character (Fig. 8) due to the stepwise expansion of the crystalline lattice [13], modulating hierarchical potential of cavitate and Zeeman splitting. In addition, the magnetic field can change the asymmetry of the density of states above and below the Fermi level, significantly affecting the current flow [14]. From the above energy diagram it is easy to see that at a voltage U higher than $\Delta E_{\perp}$ the upper edge of the conduction mini-band of one layer falls below the lower edge of the conduction mini-band of the other layer and the electrons have nowhere to move. Observed in the experiment, the regions of smooth current decay are caused by electron scattering processes. It is clear that such a simple scheme of the current flow perpendicular to the nanosheets must be supplemented by mechanisms that take into account processes of coherent magnetization of guest cavity, which will lead to magnetoelectric interactions with complex localization–relaxation processes, and take into account the conditions of resonant tunneling depending on the value of applied voltage.

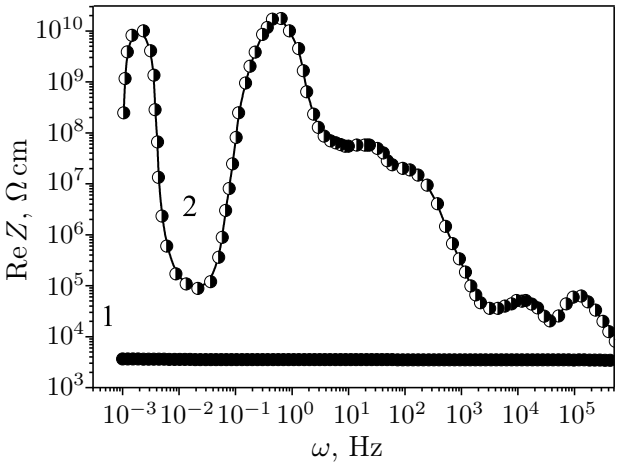

Fig. 9. Frequency dependencies of the real component of the specific complex impedance in InSe⟨β-CD⟨$FeSO_4$⟩⟩ clathrate synthesized under the electric field with simultaneous illumination. The dependencies were measured in dark (1) and in a magnetic field (2) [8].

In the case of the synthesis of the studied clathrate, while simultaneously applying a constant electric field and illumination, the VAC has a straight-line dependence, but a frequency-dependent colossal magnetoresistive effect is revealed (Fig. 9). Obviously, this structure is extremely promising for hypersensitive magnetic field sensors. In this case, the maximum increase in the resistivity reaches 10^7-fold value and the MR ratio is 99.99%.

5. Mathematical modeling

The specific crystalline structure of layered semiconductors (InSe, GaSe) is caused by different chemical bonds in different crystallographic directions: ion-covalent bonding within the layer and van der Waals between the layers. Layered materials are composed of a stack of two-dimensional (2D) layers with weak interlayer electron coupling, determined by the interlayer transfer integral t_z. Such layered structure may be of natural molecular origin, as, e.g., in cuprates, organic metals or graphite, or of artificial origin, as in heterostructure. The small value of t_z, which is much smaller than the in-plane Fermi energy E_F, provides these compounds with highly anisotropic electronic properties. Such strong anisotropy of chemical bonds also has a decisive effect on the charge carrier scattering. For example, the conductivity of such systems along or across layers is several orders of magnitude. Moreover, the anisotropy can be increased by intercalation. Intercalation in layered semiconductors of 3D transition elements allows, while maintaining the integral structure of the lattice of the base compound, to form nanometer layers with alternate magnetic and semiconductor properties.

Determination of the electronic structure of layered crystals is one of the fundamental problems of condensed matter physics. A number of recent work has been devoted to the theoretical calculation of the band electron spectrum of quasi-two-dimensional crystals [23, 24]. Information on the law of dispersion of quasi-particles is important both for understanding their physical properties and the study of electron spectrum rearrangement under the influence of intercalated impurities. In layered materials, the intercalation of impurities provides an alternative to doping, giving a unique ability to adjust the phonon frequencies and electronic band structure without interfering with the host lattice.

Magnetoresistance is traditionally used to explore the internal electron structure of metals [25–27]. Oscillations of magnetization are a thermodynamic effect that is completely determined by the density-of-states distribution. Observed in various strongly anisotropic layered compounds, which can not be described in the framework of the standard 3D theory, interlayer magnetoresistance is induced by disorder and by magnetic field component H_z for the direction perpendicular to the layers. This effect occurs in layered compounds with extremely high quasi-2D anisotropy, namely, when the interlayer transfer integral t_z is less than the cyclotron energy $\omega_c = eH_z/m^*$ and than the Landau level (LL) broadening due to impurities.

A large number of papers ([28] and references in this paper) are devoted to the study of the conductivity of quasi-two-dimensional (2D) multilayer systems in a magnetic field. The growing interest is due to: (i) the fact that the conductivity measurement is technologically implemented for almost any system; (ii) the electrical conductivity in the magnetic field is very sensitive to the parameters of the electronic structure, revealing the restructuring of the law of dispersion and geometry of the Fermi surface.

In the presence of a magnetic field H_z perpendicular to the layers, the motion in the conductive layer is quantized, then the quasiparticle dispersion can be written as

$$\varepsilon_n(p_z) = \hbar\omega_c(n + 1/2) - 2t_z \cos p_z s,$$

where s is the interlayer distance, p_z is the interlayer momentum in z direction.

Due to the Landau quantization of the 2D electron spectrum, magnetic quantum oscillations of conductivity, as well as other characteristics, arise in the magnetic field. In [7] it is shown that in a magnetic field superimposed perpendicularly to the layers, oscillations for both the imaginary component of complex impedance and for the current-voltage characteristic in a given frequency interval appear. The aim of the present paper is to study theoretically the oscillations of magnetic conductivity to explain the experimentally obtained measurement results.

We consider a multi-layered semiconductor described by the single-band tight-binding model with the nearest-neighbor hopping and the on-site delta-function-like potential. The quasi-2D layered electron system (the z direction is confined) with disorder and interaction is described by the following Hamiltonian

$$H = H_0 + H_t + H_I + H_{int}. \tag{2}$$

The first term H_0 is the Hamiltonian of the noninteracting 2D electron gas in magnetic field summed over all layers:

$$H_0 = s \int d^2r \sum_{\sigma,j} \left[\Psi^+_{j,\sigma}(\boldsymbol{r}) \left(\frac{1}{2m^*}(-i\boldsymbol{\nabla} - e\boldsymbol{A})^2 - \mu\boldsymbol{\sigma}\cdot\boldsymbol{H} \right) \Psi_{j,\sigma}(\boldsymbol{r}) \right], \tag{3}$$

where $\Psi^+_{j,\sigma}$, $\Psi_{j,\sigma}$ are the creation (annihilation) operators of an electron on the layer j at the point $\boldsymbol{r}$.

The second term in (2) gives the coherent electron tunnelling between two layers:

$$H_t = -t_s \int d^2r \sum_{\sigma,j} \Psi^+_{j,\sigma}(\boldsymbol{r})\Psi_{j+1,\sigma}(\boldsymbol{r}) \exp\Big(- ie \int_{j_s}^{(j+1)_s} A_z(\boldsymbol{r}, j, \tau)dz \Big). \tag{4}$$

This interlayer tunnelling Hamiltonian is called "coherent" because it conserves the in-layer coordinate dependence of the electron wave function (in other words, it conserves the in-plane electron momentum) after the interlayer tunnelling.

The third term describes the interaction of electrons with impurity potential $u_j(\boldsymbol{r})$:

$$H_I = s \int d^2r \sum_{\sigma,j} \Psi^+_{j,\sigma}(\boldsymbol{r}) u_j(\boldsymbol{r}) \Psi_{j,\sigma}(\boldsymbol{r}). \tag{5}$$

The impurity scattering described by this term in Hamiltonian is mainly based on perturbation theory, for example, in a self-consistent Born approximation [29]. We further discuss point-like impurities with a volume concentration n_j and two-dimensional concentration $N_j = n_j s$ in each layer. The distribution of impurities in different layers is not correlated. The potential $u_j(\boldsymbol{r})$ of each impurity at a point $\boldsymbol{r}_j$ is given by the expression $u_j(\boldsymbol{r}) = u\delta^3(\boldsymbol{r} - \boldsymbol{r}_j)$. In the case of different types of impurities, the sum by j in the equation (5) also includes different types of impurities that differ in the strength of the impurity potential u.

The last term H_{int} describes the electron-electron and electron-phonon interaction. Even without this term and for the case of point-like impurity potential, the exact solution of this Hamiltonian is not achievable [28].

In such a model, the longitudinal current density arises only from tunneling processes and is given by the expression

$$J_z(\boldsymbol{r}, j, \tau) = -\frac{\delta H_t}{\delta A_z(\boldsymbol{r}, j, \tau)} = -iets^2 \sum_{\sigma} \left(\Psi^+_{j,\sigma}(\boldsymbol{r}) \Psi_{j,\sigma}(\boldsymbol{r}) \exp(-iesA_z(\boldsymbol{r}, j, \tau)) \right). \tag{6}$$

Using the formalism of usual temperature Green's functions defined by [30]

$$G^{\sigma_1\sigma_2}_{i,j}(\boldsymbol{r}_1, \tau_1, \boldsymbol{r}_2, \tau_2) = -\langle T_\tau \Psi_{i,\sigma_1}(\boldsymbol{r}_1, \tau_1) \Psi^+_{j,\sigma_2}(\boldsymbol{r}_2, \tau_2) \rangle, \tag{7}$$

where the averaging is carried out over the grand canonical ensemble, the average current density in the j-th nanolayer in terms of Green's functions reads

$$j_j(\boldsymbol{r}, \tau) = \langle J_z(\boldsymbol{r}, j, \tau) \rangle = j^P_j(\boldsymbol{r}, \tau) + j^D_j(\boldsymbol{r}, \tau), \tag{8}$$

where we distinguish the contribution from the paramagnetic and diamagnetic components of the current density.

The equation of motion for the Green's functions in the presence of a magnetic field, impurities and vector potential $A_z(\boldsymbol{r}, j, \tau)$ for the given spin value σ is written as [29]

$$\left(-\frac{\partial}{\partial\tau} - \frac{1}{2m*}(-i\boldsymbol{\nabla} - e\boldsymbol{A})^2 + t_z(\Delta_{j+}e^{-iesA_z} + \Delta_{j-}e^{iesA_z}) + \mu + \mu_e\sigma H - u_j(\boldsymbol{r}) \right) G_{\sigma,j,l}(\boldsymbol{r}, \tau, \boldsymbol{r}', \tau') = s^{-1}\delta_{jl}\delta(\boldsymbol{r} - \boldsymbol{r}')\delta(\tau - \tau'), \tag{9}$$

where the operators $\Delta_{j+}\Psi_{j,\sigma}(\boldsymbol{r}, \tau) = \Psi_{j\pm1,\sigma}(\boldsymbol{r}, \tau)$.

The interlayer conductivity σ_{zz} of the heterosystem under the influence of the magnetic field perpendicular to the nanosheets can be written in the form

$$\sigma_{zz} = e^2 s \frac{g_0}{2} \omega_c \sum_{n,\sigma} \int \frac{dp_z}{2\pi} v_z^2(p_z) \int \frac{d\varepsilon}{2\pi} (-n'_F(\varepsilon)) \left(G^R_{\sigma,n,p_z,\varepsilon} G^A_{\sigma,n,p_z,\varepsilon} - \mathrm{Re}(G^R_{\sigma,n,p_z,\varepsilon})^2 \right), \tag{10}$$

where $n'_F(\varepsilon)$ is the derivative of the Fermi–Dirac distribution function

$$n'_F(\varepsilon) = -\frac{1}{4T\cosh^2\left(\frac{\varepsilon-\mu}{2T}\right)},$$

here T is temperature. The functions G^R and G^A are the retarded and advanced Green's functions defined by

$$G^A_{\sigma,n,p_z,\varepsilon} = \left(G^R_{\sigma,n,p_z,\varepsilon}\right)^* = \frac{1}{\varepsilon - \xi_{\sigma,n,p_z} + i\Gamma_{\varepsilon+\mu}}, \tag{11}$$

$$\xi_{\sigma,n,p_z} = \left(n + \frac{1}{2}\right)\omega_c - 2t_z \cos p_z s - \mu - \sigma\mu_e H, \tag{12}$$

where μ_e is the electron's magnetic moment, and $\Sigma(\varepsilon) = i\Gamma_\varepsilon$ is the energy-depended impurity self-

energy. It arises mainly from impurity scattering. The main contribution to resistivity comes from the short-range impurity scattering. We approximate short-range impurities by point-like ones. Then, if one does not take into account the diagrams with intersections of impurity lines in the self-energy (the contribution of such diagrams at finite k_z dispersion of electrons is usually small) the electron self-energy depends only on electron energy and not on electron quantum numbers. This fact greatly simplifies the calculations. The constant part of the real part of electron self-energy produces only a constant shift of the chemical potential. It does not influence the physical effects and, hence, is omitted in the subsequent calculations.

In the limit $\omega_c \gg 4\pi t$, the total magnetic conductivity can be written in a simpler form: the oscillating part of σ_{zz} becomes independent of the interlayer integral integral t_z, which only appears in the normalization factor σ_0 of the zero field. This clearly establishes the physical origin of the σ_{zz} oscillations as a quantization of motion in a plane perpendicular to the magnetic field, affecting the transport between the nanosheets across the energy spectrum. Then the total magnetic conductivity is given by

$$\sigma_{zz} = \int_{-\infty}^{+\infty} (-n'_F(\varepsilon - \mu))\sigma_{zz}(\varepsilon)\, d\varepsilon, \tag{13}$$

$$\frac{\sigma_{zz}(\varepsilon)}{\sigma_0} = \frac{\Gamma_0}{\Gamma_\varepsilon} \frac{\sinh\left(\alpha\frac{\Gamma_\varepsilon}{\Gamma_0}\right)}{\cosh\left(\alpha\frac{\Gamma_\varepsilon}{\Gamma_0}\right) + \cos(2\pi x)} - \alpha \frac{1 + \cosh\left(\alpha\frac{\Gamma_\varepsilon}{\Gamma_0}\right)\cos(2\pi x)}{\left(\cosh\left(\alpha\frac{\Gamma_\varepsilon}{\Gamma_0}\right) + \cos(2\pi x)\right)^2}, \tag{14}$$

where σ_0 is the conductivity in the absence of a magnetic field, Γ_0 is the imaginary part of the self-energy part at zero magnetic field, parameter $\alpha = 2\pi\Gamma_0/\omega_c$ and the renormalized energy $x = \varepsilon/\omega_c$. At zero temperature, the magnetic conductivity oscillations are given by the formula

$$\sigma_{zz} = \sigma_{zz}(\mu). \tag{15}$$

It can be seen from formula (14) that the second addition makes a negative contribution to $\sigma_{zz}(\mu)$ for $\mu \sim n\omega_c$ and positive for $\mu \sim (n + 1/2)\omega_c$. Accordingly, the magnetoconductivity minima (or magnetoresistance maxima) appear when the chemical potential lies between the Landau levels. For $\omega_c \gg 2\pi\Gamma, \mu \neq (n + 1/2)\omega_c$ the contribution from both additives is of the same order, so the total magnetoconductivity at zero temperatures vanishes periodically. The numerical analysis of the dependence $\sigma_{zz}(\varepsilon)$ is performed in two modes, depending on the value of the parameter α: (i) a low-field regime: $\omega_c < 2\pi\Gamma_0$ (or $\alpha > 1$); (ii) a high-field regime: $\omega_c > 2\pi\Gamma_0$ (or $\alpha < 1$).

The graphic dependence of the function $\sigma_{zz}(\varepsilon)$ for different values of the magnetic field at $\Gamma_0 = 0.22\,\text{meV}$ and the value of $m^* = 1.96m_e$ is shown in Fig. 10. Graphic dependence analysis reveals the appearance of a pseudogap at magnetic field values above 20 T, which corresponds to the parameter $\alpha \approx 1$, and the gap width increases with the increase of the magnetic field. Such small values of $\sigma_{zz}(\varepsilon)$ for $\alpha < 1$, respectively, lead to the appearance of a giant magnetoresistance $\rho_{zz} = \sigma_{zz}^{-1}(\varepsilon)$ at low temperatures. According to equation (13) and when $\mu \approx n\omega_c$, the main mechanism of conduction in this case is the thermal excitation of quasiparticles at the edges of the pseudogap.

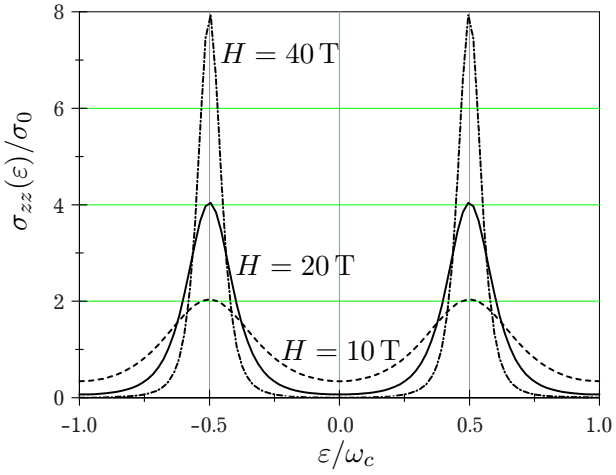

Fig. 10. Graphic dependence of $\sigma_{zz}(\varepsilon)/\sigma_0$ on the value of ε/ω_c, which detects a pseudogap at high field values. The appearance of a pseudogap at $H = 20\,\text{T}$, that is, for the value of the parameter $\alpha \approx 1$.

The two phenomena lay in the basis of the specific features of the magnetoconductivity in 2D layered heterostructure, namely Landau quantization of energy levels in magnetic fields, and the disorder-induced localization. In order to calculate the electron self-energy we use the self-consistent Born approximation [28]. It is known that the imaginary part of self-energy is proportional to the density of states:

$$g(\varepsilon) = \frac{i}{2\pi} \sum_{\sigma,n,p_z} (G^R_{\sigma,n,p_z,\varepsilon-\mu} - G^A_{\sigma,n,p_z,\varepsilon-\mu}). \tag{16}$$

Using the Poisson summation formula

$$\sum_{n=0}^{+\infty} f(n) = \sum_{l=-\infty}^{+\infty} \int_a^{+\infty} e^{-2\pi i l u} f(u)\, du,$$

which is valid for arbitrary function $f(u)$, $a \in (-1;0)$, and after summation over momentum p_z, we obtain

$$g(\varepsilon) = g_0 \left(1 + 2\sum_{l=1}^{\infty} (-1)^l J_0\left(\frac{4\pi l t}{\omega_c}\right) e^{-2\pi l \frac{\Gamma_\varepsilon}{\omega_c}} \cos\left(2\pi l \frac{\varepsilon}{\omega_c}\right)\right), \tag{17}$$

where J_0 is the zero order Bessel function, g_0 is density of states at zero magnetic field.

In the self-consistent Born approximation, neglecting multiple scattering on one impurity, a non-linear equation for unknown self-energy Γ_ε is as follows:

$$\frac{\Gamma_\varepsilon}{\Gamma_0} = 1 + \frac{\sinh(\alpha\Gamma_\varepsilon/\Gamma_0)}{\cosh(\alpha\Gamma_\varepsilon/\Gamma_0) + \cos(2\pi x)}. \tag{18}$$

Beyond the Born approximation the relation (18) is no more valid as other scattering mechanisms should be taken into account.

Now, let us discuss other limitations of proposed theoretical analysis. First of all, we considered the case of small values of the interlayer transfer integral, namely, when t_z is less than the cyclotron energy and than the LL's broadening Γ_0 due to impurities. In the other case, the electron interlayer jumps and electron scattering on impurities should not be considered separately. The other limitation is that magnetic field has the direction perpendicular to the layers. A finite tilt angle of the magnetic field may be approximately taken into account by re-scaling the LL's separation. In this paper we considered short-range impurities, the generalisation of the obtained results for the case of screened Coulomb impurities that is expected to be particularly relevant experimentally is addressed to future work.

6. Conclusion

1. The hierarchization of InSe$\langle\beta$-CD$\langle$FeSO$_4\rangle\rangle$ structure results not only in the expansion of the initial matrix but also in the decreasing of interlayer distance in non-intercalated areas of a nanostructure. The essentially different variation character of the real component of the complex impedance is due to the delocalized charge carriers in the initial matrix, in comparison with the case of clathrate synthesis under the normal conditions. The hopping mechanism of conductivity gives a significant contribution to the current conduction due to the concentration of trap centers in the vicinity of the Fermi level.

2. The response to a constant magnetic field applied normally to the nanolayers is accompanied by a cardinal transformation of the frequency dependences $\mathrm{Re}\, Z(\omega)$ and the Nyquist diagrams only for the structures synthesized in the electric field under the simultaneous illumination. In particular, there appears a strong inductive response in the low-frequency interval. At the same time, unlike the behavior of a nanohybrid synthesized under the normal conditions, the magnetoresistive effect, in this case, depends on the frequency and can demonstrate a giant (almost 10^7) growth at room temperature.

3. The influence of the magnetic field causes both a reduction of the conductivity associated with delocalized charge carriers and a growth of the hopping conductivity, as well as the quantization of energy levels of charge carriers, in particular, in impurity subbands, which can result in the oscillatory behavior of the real component of the impedance in the low-frequency interval.

4. The theoretical model is developed to describe the interlayer magnetoconductivity in InSe⟨β-CD⟨$FeSO_4$⟩⟩ heterostructure in strongly anisotropic 2D compounds. The Hamiltonian model describes the noninteracting 2D electron gas in a magnetic field, the coherent electron tunneling between layers, and the electron interaction with impurity potential.

5. The analytical expressions are given for the magnetoconductivity in the layered compounds in presence of a quantizing magnetic field perpendicular to the layers and for short-range impurity scattering in the frame of quantum transport theory. The electron scattering only on short-range impurities is taken into account in the frames of the self-consistent Born approximation.

6. Graphic dependencies of oscillating magnetoconductivity are analysed for different values of a quantizing magnetic field in a layered structure whose interlayer transfer integral can be controlled artificially.

7. The thermally activated behavior of the magnetoconductivity minima that occur when chemical potential is between the Landau levels is in agreement with the experimental observation of giant magnetoresistance maxima, reaching 10^7-fold values at low temperatures. The results of both theoretical calculation and controllable experiments show the well qualitative and quantitative agreements of the proposed theory with experiments in very anisotropic layered heterostructures.

[1] Baibich M. N., Broto J. M., Fert A., Nguyen Van Dau, Petroff F., Etienne P., Creuzet G., Friederich A., Chazelas J. Giant magnetoresistance of (001)Fe/(001)Cr magnetic superlattices. Physical Review Letters. **61** (21), 2472–2475 (1988).

[2] Binasch G., Grunberg P., Saurenbach F., Zinn W. Enhanced magnetoresistance in layered magnetic structures with antiferromagnetic interlayer exchange. Physical Review B. **39** (7), 4828–4830 (1989).

[3] Prinz G. Magnetoelectronics. Science. **282** (5394), 1660–1663 (1998).

[4] Wolf S. A., Awschalom D. D., Buhrman R. A., Daughton J. M., von Molnár S., Roukes M. L., Chtchelkanova A. Y., Treger D. M. Spintronics: a spin-based electronics vision for the future. Science. **294** (5546), 1488–1495 (2001).

[5] Ross C. A. Patterned magnetic recording media. Annual Review of Materials Research. **31**, 203–235 (2001).

[6] Daughton J. M., Pohm A. V., Fayfield R. T., Smith C. H. Applications of spin dependent transport materials. Journal of Physics D: Applied Physics. **32** (22), R169–R177 (1999).

[7] Ivashchyshyn F. O., Grygorchak I. I., Klapchuk M. I. Impedance anisotropy and quantum photocapacity of bio/inorganic clathrates InSe⟨histidine⟩ and GaSe⟨histidine⟩. Nanosystems, Nanomaterials, nanotechnologies. **13** (3), 403–414 (2015).

[8] Grygorchak I. I., Hryhorchak O. I., Ivashchyshyn F. O. Modification of the properties of InSe⟨β-CD⟨$FeSO_4$⟩⟩ clathrate/cavitate complexes with hierarchical architecture at their synthesis in crossed electric and light-wave fields. Ukrainian Journal of Physics. **62** (7), 625–632 (2017).

[9] Kostrobij P., Grygorchak I., Ivashchyshyn F., Markovych B., Viznovych O., Tokarchuk M. Generalized Electrodiffusion Equation with Fractality of Space-Time: Experiment and Theory. J. Phys. Chem. A. **122** (16), 4099–4110 (2018).

[10] Lehn J. M. Supramolecular Chemistry: Concepts and Perspectives. Berlin, Wiley-VCH Verlag GmbH (1995).

[11] Grygorchak I. I. at al. Fizychni procesy u supramolekulyarnyx ansamblyax ta yix praktychne zastosuvannya: monohrafiya. Chernivci, Cherniv. nac. universytet (2016), (in Ukrainian).

[12] Steed J., Atwood J. Supramolecular Chemistry. John Wiley and Sons (2009).

[13] Savitskii P. I., Mintyanskii I. V., Kovalyuk Z. D. Anizotropiya elektroprovodnosti v monoselenide indiya. Neorganicheskije materialy. **32** (4), 405–409 (1996), (in Russian).

[14] Savitskii P. I., Mintyanskii I. V., Kovalyuk Z. D. Annealing effect on conductivity anisotropy in indium selenide single crystals. Physica Status Solidi (a). **155** (2), 451–460 (1996).

[15] Savitskii P. I., Kovalyuk Z. D., Mintyanskii I. V. Termostimulirovannoe izmenenie sostoyaniya defektov v monoselenide indiya. Neorganicheskije materialy. **33** (9), 1062–1066 (1997), (in Russian).

[16] Savitskii P. I., Kovalyuk Z. D., Mintyanskii I. V. Space-charge region scattering in indium monoselenide. Physica Status Solidi (a). **180** (2), 523–531 (2000).

[17] Mushinskii V. P., Karaman M. I. Opticheskie svojstva hal'kogenidov galliya i indiya. Kishinev, MUSSR: Shtiinca (1973), (in Russian).

[18] Landot-Bornstein. Numerical data and functional relationships in science and technology. Ed. A. Mashke. Berlin, Springer-Verlag (1999).

[19] Friend R. H., Yoffe A. D. Electronic properties of intercalation complexes of the transition metal dichalcogenides. Advances in Physics. **36** (1), 1–94 (1987).

[20] Grygorchak I., Ivashchyshyn F., Stakhira P., Reghu R. R., Cherpak V. Intercalated nanostructure consisting of inorganic receptor and organic ambipolar semiconductor. Journal of Nanoelectronics and Optoelectronics. **8** (3), 292–296 (2013).

[21] Stojnov Z. B., Grafov B. M., Savova-Stojnova B., Elkin V. V. Elektrohimicheskij impedans. Moskva, Nauka (1991), (in Russian).

[22] Barsoukov E., Macdonald J. R. Impedance spectroscopy. Theory, experiment and application. Wiley Interscience (2005).

[23] Stasyuk I. V., Velychko O. V. The study of electronic states in highly anisotropic layered structures with stage ordering. Journal of Physical Studies. **18** (2/3), 2002-1–2002-9 (2014).

[24] Stasyuk I. V., Velychko O. V. Electron spectrum of intercalated stage ordered layered structures: periodic Anderson model approach. Mathematical Modeling and Computing. **2** (2), 191–203 (2015).

[25] Ziman J. M. Principles of the Theory of Solids. Cambridge, Cambridge University Press (1972).

[26] Abrikosov A. A. Fundamentals of the Theory of Metals. Amsterdam, New York, North-Holland (1988).

[27] Shoenberg D. Magnetic Oscillations in Metals. Cambridge, Cambridge University Press (1984).

[28] Grigoriev P. The influence of the chemical potential oscillations on the de Haas-van Alphen effect in quasi-two-dimensional compounds. Journal of Experimental and Theoretical Physics. **92**, 1090–1094 (2001).

[29] Champel T., Mineev V. Magnetic quantum oscillations of the longitudinal conductivity σ_{zz} in quasi two-dimensional Metals. Physical Review B. **66** (19), 195111 (2003).

[30] Abrikosov A. A., Gorkov L. P., Dzyaloshinski I. E. Methods of Quantum Field Theory in Stastistical Physics. New Jersey, Prentice Hall (1964).

Гігантський магнеторезистивний ефект в клатраті InSe⟨β-CD⟨$FeSO_4$⟩⟩

Клапчук М. І.[1], Іващишин Ф. О.[1,2]

[1] *Національний університет "Львівська політехніка", вул. С. Бандери, 12, 79013, Львів, Україна*
[2] *Ченстоховський технологічний університет, вул. Армії Крайової, 17, 42-200, Польща*

Клатрат InSe⟨β-CD⟨$FeSO_4$⟩⟩ з ієрархічною архітектурою виявляє гігантський магніторезистивний ефект та надзвичайну (осциляційну) поведінку вольт-амперної характеристики в магнітному полі у напрямку, перпендикулярному до наношарів. Запропоновано новий технологічний підхід до синтезу багатошарової наноструктури. Це дозволяє досягти чотириразового ступеня розширення початкової InSe напівпровідникової матриці, в якій кавітат β-циклодекстрину (β-CD) і сульфат заліза слугує гостьовим компонентом. Це дає можливість розробити теоретичну модель для опису міжшарової магнетопровідності в такій надзвичайно анізотропній двошаровій сполуці. Аналізуються графічні залежності осциляційної магнетопровідності для різних значень квантуючого магнітного поля в шаруватій структурі, в якій міжшаровий інтеграл перескоку може бути контрольований штучно.

Ключові слова: *селенід індію, клатрат, ієрархічні структури, імпедансна спектроскопія, гігантський магніторезистивний ефект.*